

Effect of thermal gradients on stress/strain distributions in a thin circular symmetric plate

Nelli N. Aleksandrova*

Centre of Exact Sciences and Engineering, Madeira University, 9020-105 Funchal, Madeira, Portugal

(Received September 30, 2015, Revised February 11, 2016, Accepted February 13, 2016)

Abstract. The analysis of thermally induced stresses in engineering structures is a very important and necessary task with respect to design and modeling of pressurized containers, heat exchangers, aircrafts segments, etc. to prevent them from failure and improve working conditions. So, the purpose of this study is to investigate elasto-plastic thermal stresses and deformations in a thin annular plate embedded into rigid container. To this end, analytical research devoted to mathematically and physically rigorous stress/strain analysis is performed. In order to evaluate the effect of logarithmic thermal gradients, commonly applied to structures which incorporate thin plate geometries, different thermal parameters such as temperature mismatch and varying constraint temperature were introduced into the model of elastic perfectly-plastic annular plate obeying the von Mises yield criterion with its associated flow rule. The results obtained may be used in sensitive to temperature differences aircraft structures where the thermal effects on equipment must be kept in mind.

Keywords: logarithmic thermal gradient; plane stress; perfect plasticity; analytical solution

1. Introduction

Annular plates embedded into rigid containers are versatile models for many civil, mechanical, aeronautical, marine and chemical engineering applications (Ventsel and Krauthammer 2001), especially useful for pressure vessels, heat exchangers, aircraft segments, and loose-material containers. In structural mechanics these applications particularly include various types of structural steel or aluminum members working in varying temperature ambient. Design of a common structure to minimize the thermal stresses for a given temperature distribution usually tends to cause loss of strength and stiffness of its members, a loss which has to be rectified by addition of extra material. In fact, reduction of thermal stresses by choice of another material is possible only to a limited extent. If one material is the most suitable on mechanical grounds and is able to withstand the required temperatures, one would be reluctant to abandon it because of thermal stresses. Hence, when the weight penalty is crucial for structural performance such as in aircraft industry, the detailed analysis of temperature induced stresses and related deformations is of great demand.

For this reason, the classical problem of thin annular plate (to admit plane-stress solution which

*Corresponding author, Professor, E-mail: nelli@staff.uma.pt

is most suitable for specific engineering applications) subjected to thermal fields has been the topic of a variety of theoretical investigations. It is treated in a purely thermo-elastic stress state by Timoshenko and Goodier (1970), Ugural and Fenster (2012); and in the thermo-elasto-plastic stress state by Alexandrov (2015).

Temperature fields which are suitable for modeling structural engineering applications in a preliminary design stage may be divided into two types: uniform temperature distributions and steady state temperature distributions (logarithmic or linear). Based on the uniform temperature distribution and Tsai-Hill yield criterion, Sen and Sayer (2006) carried out numerical elasto-plastic thermal stress-strain analysis in a composite disk. Since the composite disk has different thermal expansion coefficients in radial and tangential directions, thermal stresses were produced in it by the applied uniform temperature loading. The obtained results showed that the thermal stresses were considerably affected by increasing temperature values. Within the same uniform temperature assumption and von Mises yield criterion, thermal effects on the development of plastic zones in thin annular axisymmetric plates were investigated by Alexandrov and Alexandrova (2001). However, here the thermal stresses were due to displacement constraints applied at the outer radius of the plate. It was shown that the plate becomes fully plastic at an insignificant rise of temperature from the beginning of plastic flow. Recently, the combined effect of uniform temperature field and inner pressure loading on the plastic collapse mechanism of thin annular constrained (at the outer radius) plates was studied by Alexandrov and Pham (2014) based on the Hill's quadratic orthotropic yield criterion. It was shown that two different plastic collapse mechanisms may occur depending on loading combinations, namely, localization of plastic strain at the inner radius of the plate or/and loss of load carrying capacity (when the plate reaches fully plastic state). For the same plate geometry, the effect of temperature-dependent mechanical properties such as yield stress, modulus of elasticity, thermal expansion coefficient and Poisson ratio on the load carrying capacity of steel plates was investigated by Alexandrov *et al.* (2014). It was shown that this effect is more pronounced for higher temperatures and smaller inner radii. The importance of temperature dependence of material properties in successful engineering design was also earlier outlined by Zabaras *et al.* (1987), Zhu and Chao (2002). However, it was revealed (Zhu and Chao 2002) that, at least for aluminum structures, all thermal and mechanical properties, except for the yield stress, can be simply taken as the room temperature values. Only the assumption of constant yield stress overestimates the material yield ability whereas the real yield stress actually reduces with increasing temperature. As concerning spatial temperature profile, it was shown (Zabaras *et al.* 1987) that the radial temperature gradient dominates over the axial one such that the axial temperature gradient may be assumed to be negligible.

To this end, for constrained thin structures, both the effect of rigid constraints and radial temperature gradients on stress/strain performance of the structure should be included in the analysis. The temperature gradient in terms of steady state temperature distribution has been studied extensively for thick cylinders and related engineering applications both in purely elastic (Timoshenko and Goodier 1970, Harvey 1985, Vullo 2014) and partially plastic stress states (obeying the Tresca yield criterion with its associated flow rule) (Bland 1956, Chakrabarty 2006, Eraslan and Apatay 2008).

So, the purpose of this research is to extend the previous work (Alexandrov and Alexandrova 2001) by including steady state temperature distributions and derive complete analytical stress/strain solution which predicts development of plastic zones in the constrained annular plate. The material of the plate is assumed to be elastic perfectly-plastic obeying the von Mises yield criterion with its associated flow rule to avoid the drawbacks of piecewise nature of the Tresca

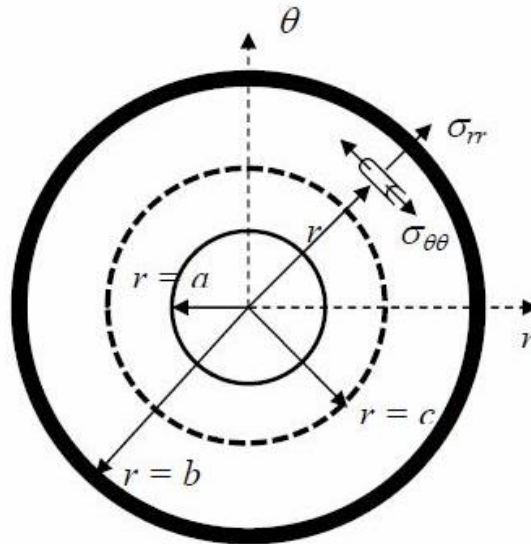


Fig. 1 Geometrical model of an annular plate embedded into rigid container

yield criterion and improve the solution in this way.

2. General equations of the problem

The unrestrained structural segment expands or contracts in proportion to temperature variation freely. But the imposed constraints may prevent the material from flow and, as a consequence, the thermal stresses develop in the constrained structural member. In cylindrical coordinate system $r\theta z$ with non-zero radial, $\hat{\sigma}_{rr}$, and circumferential, $\hat{\sigma}_{\theta\theta}$, stress tensor components, let's consider an annular plate of inner radius a and outer radius b embedded into a rigid container (Fig. 1).

Then, one of the most prevalent cases of thermal stresses occurs when heat is flowing between the sides of the structure in a steady manner causing the temperature differences between the inner and outer radii to remain constant, that is the temperature, T , satisfies the Laplace equation $\nabla^2 T=0$, the solution to which may be written as

$$T = T_b + (T_a - T_b) \frac{\ln(b/r)}{\ln(b/a)} \tag{1}$$

where T_a and T_b are the temperatures at the inner and outer surfaces, respectively. Similar logarithmic temperature distributions were also considered by Bland (1956), Timoshenko and Goodier (1970), Harvey (1985), Chakrabarty (2006), and Eraslan and Apatay (2008). Fig. 2 shows various combinations of a fixed temperature at the outer radius, T_b , and corresponding temperature mismatch, $\delta T=T_a-T_b$, for the case $b/a=2$ and $T_a>0$. It is assumed that the yield criterion and the plastic stress-strain relations are unaffected by the variation in temperature, provided the variation is not large enough to change the material properties appreciably. It is both the boundary constraint and the temperature drop throughout the width of the plate that give rise to the thermal stresses. So, the following mixed boundary conditions should be satisfied

$$\hat{\sigma}_{rr} = 0 \quad \text{at } r = a \quad (2)$$

and

$$\hat{u} = 0 \quad \text{at } r = b \quad (3)$$

where $\hat{u} = 0$ is the radial displacement. Thermal effects are then included in the constrained plate problem by the standard modification of the elastic stress-strain equations (Timoshenko and Goodier 1970) taking into account plane-stress state geometry, $\hat{\sigma}_{zz} = 0$. If the coefficient of thermal expansion is denoted by α , the dilatation produced by a rise in temperature T is equal to αT , and the general thermo-elastic stress-strain-temperature relations take the following form

$$\hat{\sigma}_{rr} = A - \frac{Bb^2}{r^2} - \frac{E\alpha}{r^2} \int_a^r T r dr, \quad \hat{\sigma}_{\theta\theta} = A + \frac{Bb^2}{r^2} + \frac{E\alpha}{r^2} \int_a^r T r dr - E\alpha T \quad (4)$$

$$\hat{u} = \frac{1}{E} \left[(1-\nu)Ar + (1+\nu)\frac{Bb^2}{r} \right] + (1+\nu)\frac{\alpha}{r} \int_a^r T r dr \quad (5)$$

after satisfying the requirement of mechanical equilibrium

$$\frac{d\hat{\sigma}_{rr}}{dr} + \frac{\hat{\sigma}_{rr} - \hat{\sigma}_{\theta\theta}}{r} = 0 \quad (6)$$

strain-displacement relations

$$\hat{\varepsilon}_{rr} = d\hat{u}/dr, \quad \hat{\varepsilon}_{\theta\theta} = \hat{u}/r \quad (7)$$

and generalized Hooke's law

$$\hat{\varepsilon}_{rr} = (\hat{\sigma}_{rr} - \nu\hat{\sigma}_{\theta\theta})\frac{1}{E} + \alpha T, \quad \hat{\varepsilon}_{\theta\theta} = (\hat{\sigma}_{\theta\theta} - \nu\hat{\sigma}_{rr})\frac{1}{E} + \alpha T \quad (8)$$

where E is the Young's modulus, ν is the value of Poisson's ratio; A , B are the constant of integrations determined from the appropriate boundary conditions; $\hat{\varepsilon}_{rr}$ and $\hat{\varepsilon}_{\theta\theta}$ are the radial and tangential strains, respectively.

To deal with the partially plastic state, the von Mises yield criterion is adopted. For plane stress state and in the absence of in-plane shear stresses, it simplifies to

$$\hat{\sigma}_{rr}^2 + \hat{\sigma}_{\theta\theta}^2 - \hat{\sigma}_{rr}\hat{\sigma}_{\theta\theta} = Y^2 \quad (9)$$

and is automatically satisfied by the following parametric substitution

$$\hat{\sigma}_{rr}/Y = (2/\sqrt{3})\cos\varphi, \quad \hat{\sigma}_{\theta\theta}/Y = (2/\sqrt{3})\cos(\varphi - \pi/3) \quad (10)$$

where Y is the yield stress in tension and φ is an auxiliary variable. In partially plastic state, the plastic zone propagates up to some unknown radius c which should be determined in the course of the solution.

Due to the circular symmetry of the problem and plane stress assumption, $\hat{\sigma}_{rr} = \hat{\sigma}_{rr}(r)$, $\hat{\sigma}_{\theta\theta} = \hat{\sigma}_{\theta\theta}(r)$, $\hat{\sigma}_{zz} = 0$, there is only one non-trivial equilibrium Eq. (6) which is invalid both in

elastic and plastic zones.

3. Thermo-elastic solution and initiation of plastic flow

To conduct further analysis, the dimensionless parameters may be introduced at this point:
 $\sigma_{rr} = \hat{\sigma}_{rr}/Y, \sigma_{\theta\theta} = \hat{\sigma}_{\theta\theta}/Y; \beta = r/b, r_0 = a/b, \gamma = c/b; \tilde{E} = E/Y, \varepsilon_{rr} = \hat{\varepsilon}_{rr}\tilde{E}, \varepsilon_{\theta\theta} = \hat{\varepsilon}_{\theta\theta}\tilde{E};$
 $u = \hat{u}\tilde{E}/b; T_\beta = \tilde{E}(\alpha T_b)/2, \Delta T = \tilde{E}(\alpha \delta T)/2.$

Then, combining Eqs. (1)-(5), the purely thermo-elastic states are described by

$$\sigma_{rr} = A \left(1 - \frac{r_0^2}{\beta^2} \right) - I_1(\beta) \frac{1}{\beta^2}; \quad \sigma_{\theta\theta} = A \left(1 + \frac{r_0^2}{\beta^2} \right) + I_1(\beta) \frac{1}{\beta^2} - 2I_2(\beta) \quad (11)$$

$$u = \frac{A}{\beta} \left[\beta^2(1-\nu) + r_0^2(1+\nu) \right] + \frac{1}{\beta} (1+\nu) I_1(\beta); \quad A = -I_1(1)(1+\nu) / \left[r_0^2(1+\nu) + (1-\nu) \right] \quad (12)$$

where here and later on

$$I_1(\beta) = T_\beta (\beta^2 - r_0^2) + \frac{\Delta T}{\ln r_0} \left[\beta^2 \left(\ln \beta - \frac{1}{2} \right) - r_0^2 \left(\ln r_0 - \frac{1}{2} \right) \right]; \quad I_2(\beta) = T_\beta + \Delta T \frac{\ln \beta}{\ln r_0} \quad (13)$$

For sufficiently small values of temperature, the whole plate is entirely elastic. The elastic carrying capacity (when the plate starts yielding) may then be determined by substitution of Eq. (11) into Eq. (9) observing that the initial yield starts from the inner edge of the plate (where the left hand side of Eq. (9) attains its maximum).

For higher temperatures, the plate in general consists of two zones-inner plastic (which will be denoted by upper index “ P_z ”) and outer elastic (which will be denoted by upper index “ E ”)—divided by the elastic/plastic boundary, γ .

In the outer elastic zone, one has boundary condition in displacement (3): $u=0$ at $\beta=1$. Then, from Eqs. (4)-(5), the stresses and displacement become

$$\sigma_{rr}^E = A \left(1 + \frac{1-\nu}{1+\nu} \frac{1}{\beta^2} \right) + \left[I_1(1) - I_1(\beta) \right] \frac{1}{\beta^2}, \quad (14)$$

$$\sigma_{\theta\theta}^E = A \left(1 - \frac{1-\nu}{1+\nu} \frac{1}{\beta^2} \right) - \left[I_1(1) - I_1(\beta) \right] \frac{1}{\beta^2} - 2I_2(\beta)$$

$$u^E = A(1-\nu) \left(\beta - \frac{1}{\beta} \right) - \frac{1}{\beta} (1+\nu) \left[I_1(1) - I_1(\beta) \right] \quad (15)$$

where functions I_1 and I_2 are defined by Eq. (13), and the constant of integration A (together with the radius of propagation of plastic zone) should be determined from the stress continuity conditions at the elastic-plastic boundary γ

$$\sigma_{rr}^P(\gamma) - \sigma_{rr}^E(\gamma) = 0, \quad \sigma_{\theta\theta}^P(\gamma) - \sigma_{\theta\theta}^E(\gamma) = 0 \quad (16)$$

4. Plastic solution for stresses in the plastic zone

In the inner plastic zone, the stress state is defined by Eq. (10) which is in dimensionless form may be rewritten as

$$\sigma_{rr}^P = (2/\sqrt{3})\cos\varphi, \quad \sigma_{\theta\theta}^P = (2/\sqrt{3})\cos(\varphi - \pi/3) \quad (17)$$

Substitution of Eq. (17) into the equilibrium Eq. (6) leads to an analytical expression defining the relation between the radial coordinate β and auxiliary variable φ

$$\beta = r_0 \frac{\sqrt{|\sin(\varphi_\alpha - \pi/6)|}}{\sqrt{|\sin(\varphi - \pi/6)|}} \exp\left[\frac{\sqrt{3}}{2}(\varphi_\alpha - \varphi)\right] \quad (18)$$

where φ_α is the value of φ at $\beta=r_0$, and is obtained from the boundary condition in stress (2): $\sigma_{rr}^P = 0$ at $\beta=r_0$ such as $\varphi_\alpha = -\pi/2$.

So, substitution of Eqs. (14) and (17) into Eq. (16) gives two final equations: one for constant A to complete stress/strain fields (14), (15) in the outer elastic zone

$$A = I_2(\gamma) + \cos(\varphi_\gamma - \pi/6) \quad (19)$$

and another-for an auxiliary function φ_γ (the value of φ at the elastic-plastic boundary γ)

$$\frac{2}{1+\nu} T_\beta \frac{1}{\gamma^2} + \frac{\Delta T}{\ln r_0} \left[\frac{1}{\gamma^2} \left(\frac{1-\nu}{1+\nu} \ln \gamma - \frac{1}{2} \right) + \frac{1}{2} \right] = \frac{2}{\sqrt{3}} \cos \varphi_\gamma - \left(1 + \frac{1-\nu}{1+\nu} \frac{1}{\gamma^2} \right) \cos \left(\varphi_\gamma - \frac{\pi}{6} \right) \quad (20)$$

Eq. (20) directly leads to the determination of the plastic border radius γ taking into account Eq. (18) rewritten for this purpose in the form

$$\frac{1}{\gamma^2} = \frac{1}{r_0^2} \frac{|\sin(\varphi_\gamma - \pi/6)|}{|\sin(\varphi_\alpha - \pi/6)|} \exp\left[-\sqrt{3}(\varphi_\alpha - \varphi_\gamma)\right] \quad (21)$$

5. Kinematic analysis for temperature gradient loaded plates

According to the mathematically and physically rigorous procedure exploited in the present research, the total strain in the inner plastic zone is assumed to be the sum of thermo-elastic and plastic portions. The thermo-elastic portion is obtained from the Hooke's law (8) and stress distributions (10)

$$\begin{aligned} \varepsilon_{rr}^e &= \left[(2-\nu)\cos\varphi - \sqrt{3}\nu\sin\varphi \right] \sqrt{3} + 2I_2(\beta), \\ \varepsilon_{\theta\theta}^e &= \left[(1-2\nu)\cos\varphi + \sqrt{3}\sin\varphi \right] \sqrt{3} + 2I_2(\beta) \end{aligned} \quad (22)$$

where β as a function of φ is given by Eq. (18) with $\varphi_\alpha = -\pi/2$. The plastic portion is related to the associated (with the Mises yield criterion (9)) flow rule

$$\dot{\varepsilon}_{rr}^P / \dot{\varepsilon}_{\theta\theta}^P = s_{rr} / s_{\theta\theta} \quad (23)$$

where $\dot{\varepsilon}_{rr}^p$ and $\dot{\varepsilon}_{\theta\theta}^p$ are the radial and tangential plastic portions of strain rate tensor components, respectively; s_{rr} and $s_{\theta\theta}$ are the radial and circumferential deviatoric components of stress tensor, respectively. At small strains, $\dot{\varepsilon}_{rr}^p = \partial\varepsilon_{rr}^p/\partial t$ and $\dot{\varepsilon}_{\theta\theta}^p = \partial\varepsilon_{\theta\theta}^p/\partial t$, where ε_{rr}^p and $\varepsilon_{\theta\theta}^p$ are the radial and tangential plastic portions of strains, respectively, and t is a time factor. It follows from Eqs. (10) and (18) that the deviatoric components of stresses are independent of time. Therefore, Eq. (23) may be immediately integrated to give

$$\varepsilon_{rr}^p = \varepsilon_{\theta\theta}^p (\sqrt{3} \cos \varphi - \sin \varphi) / (2 \sin \varphi) \tag{24}$$

Due to the general statement of the problem, in the plastic zone $\varepsilon_{rr}^{Pz} = \varepsilon_{rr}^e + \varepsilon_{rr}^p = \partial u^{Pz} / \partial \beta$ and $\varepsilon_{\theta\theta}^{Pz} = \varepsilon_{\theta\theta}^e + \varepsilon_{\theta\theta}^p = u^{Pz} / \beta$. Substituting Eqs. (22) and (24) into these equalities gives

$$\begin{aligned} \frac{\partial u^{Pz}}{\partial \beta} &= \frac{1}{\sqrt{3}} [(2 - \nu) \cos \varphi - \sqrt{3} \nu \sin \varphi] + 2I_2(\beta) + \varepsilon_{\theta\theta}^p \frac{\sqrt{3} \cos \varphi - \sin \varphi}{2 \sin \varphi}, \\ \frac{u^{Pz}}{\beta} &= \frac{1}{\sqrt{3}} [(1 - 2\nu) \cos \varphi + \sqrt{3} \sin \varphi] + 2I_2(\beta) + \varepsilon_{\theta\theta}^p \end{aligned} \tag{25}$$

Elimination of $\varepsilon_{\theta\theta}^p$ from Eq. (25) results in differential equation for radial displacement in the plastic zone

$$\frac{\partial u^{Pz}}{\partial \beta} + \frac{\sin(\varphi - \pi/3)}{\sin \varphi} \frac{u^{Pz}}{\beta} = \frac{1 - 2\nu}{2\sqrt{3} \sin \varphi} (\sin 2\varphi - \sqrt{3} \cos 2\varphi) + I_2(\beta) \frac{2\sqrt{3} \sin(\varphi - \pi/6)}{\sin \varphi} \tag{26}$$

which may be rewritten in terms of derivative with respect to variable φ

$$\frac{du^{Pz}}{d\varphi} - \frac{\sin(\varphi - \pi/3)}{\sin(\varphi - \pi/6)} u^{Pz} = -\frac{(1 - 2\nu)}{2\sqrt{3}} \frac{(\sin 2\varphi - \sqrt{3} \cos 2\varphi)}{\sin(\varphi - \pi/6)} \beta - 2\sqrt{3} I_2(\beta) \beta \tag{27}$$

This equation may be resolved analytically to give

$$\begin{aligned} u^{Pz}(\varphi) &= \frac{C \exp[\sqrt{3}(\varphi - \pi/6)/2]}{\sqrt{|\sin(\varphi - \pi/6)|}} - r_0 \frac{\sqrt{|\sin(\varphi_\alpha - \pi/6)|}}{\sqrt{|\sin(\varphi - \pi/6)|}} \exp[\sqrt{3}(\varphi_\alpha + \varphi)/2] \times \\ &\times \left[\frac{1 - 2\nu}{2\sqrt{3}} \int_{\varphi_\gamma}^{\varphi} \Phi_1(\varphi) d\varphi + 2\sqrt{3} \int_{\varphi_\gamma}^{\varphi} \left[T_\beta + \frac{\Delta T}{\ln r_0} \Phi_2(\varphi) \right] \exp[-\sqrt{3}\varphi] d\varphi \right] \end{aligned} \tag{28}$$

where C is a constant and

$$\begin{aligned} \Phi_1(\varphi) &= \frac{\sin 2\varphi - \sqrt{3} \cos 2\varphi}{\sin(\varphi - \pi/6)} \exp[-\sqrt{3}\varphi] \\ \Phi_2(\varphi) &= \ln r_0 + \ln \frac{\sqrt{|\sin(\varphi_\alpha - \pi/6)|}}{\sqrt{|\sin(\varphi - \pi/6)|}} + \frac{\sqrt{3}}{2} (\varphi_\alpha - \varphi) \end{aligned}$$

Since the radial displacement u is a continuous function across the elastic-plastic boundary, the

constant C in Eq. (28) may be determined from the continuity condition for displacements

$$u^P_z(\varphi_\gamma) = u_\gamma \tag{29}$$

here u_γ is the value of u at the elastic-plastic border γ , and is obtained from Eqs. (15), (19) by putting $\beta = \gamma$

$$u_\gamma = \gamma \left\{ (1-\nu) \left(1 - \frac{1}{\gamma^2} \right) \left[I_2(\gamma) + \cos(\varphi_\gamma - \pi/6) \right] - (1+\nu) \frac{1}{\gamma^2} \left[I_1(1) - I_1(\gamma) \right] \right\} \tag{30}$$

Combining Eqs. (28)-(30) yields the constant C in Eq. (28)

$$C = u_\gamma \sqrt{\sin(\varphi_\gamma - \pi/6)} \exp \left[-\frac{\sqrt{3}}{2} \left(\varphi_\gamma - \frac{\pi}{6} \right) \right] \tag{31}$$

where u_γ is given by Eq. (30); φ_γ and γ are calculated from Eqs. (20)-(21); $\varphi_\alpha = -\pi/2$.

As soon as the displacement in the plastic zone is obtained, the total tangential strain in this zone follows directly from Eq. (28) dividing u^P_z by dimensionless radius β . The elastic portion of tangential strain is given by Eq. (22)₂ where φ as a function of β is in turn given by Eq. (18). Then, the plastic portion of tangential strain is defined as the difference between the total strain and the elastic portion. Knowing the plastic portion of tangential strain, the corresponding plastic portion of radial strain is obtained by Eq. (24) and the elastic portion-by Eq. (22)₁, both with the help of Eq. (18). In the plastic zone the coordinate β goes up to the elastic-plastic border γ which is defined for specific values of temperature parameters T_β , ΔT and geometric ratio r_0 by Eqs. (20)-(21).

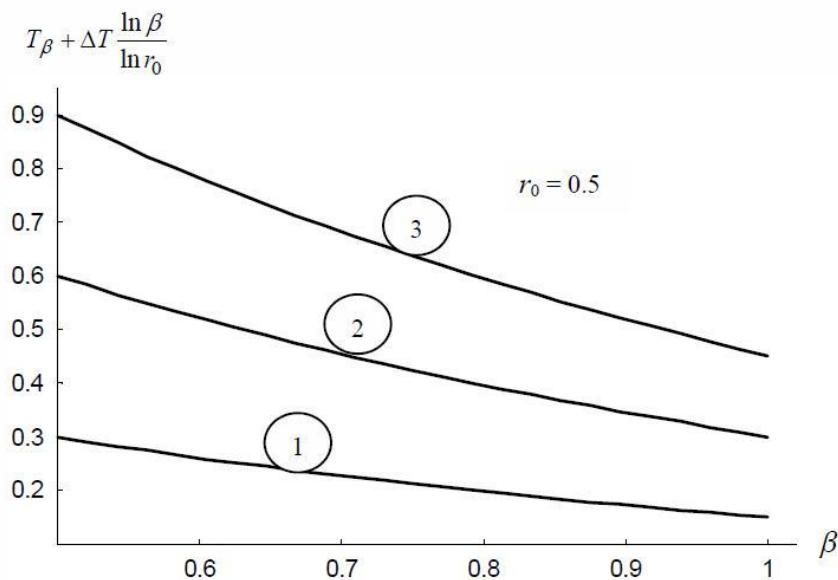


Fig. 2 Logarithmic temperature gradient field for several variations of temperature parameters: 1- $T_\beta = \Delta T = 0.15$; 2- $T_\beta = \Delta T = 0.3$; 3- $T_\beta = \Delta T = 0.45$

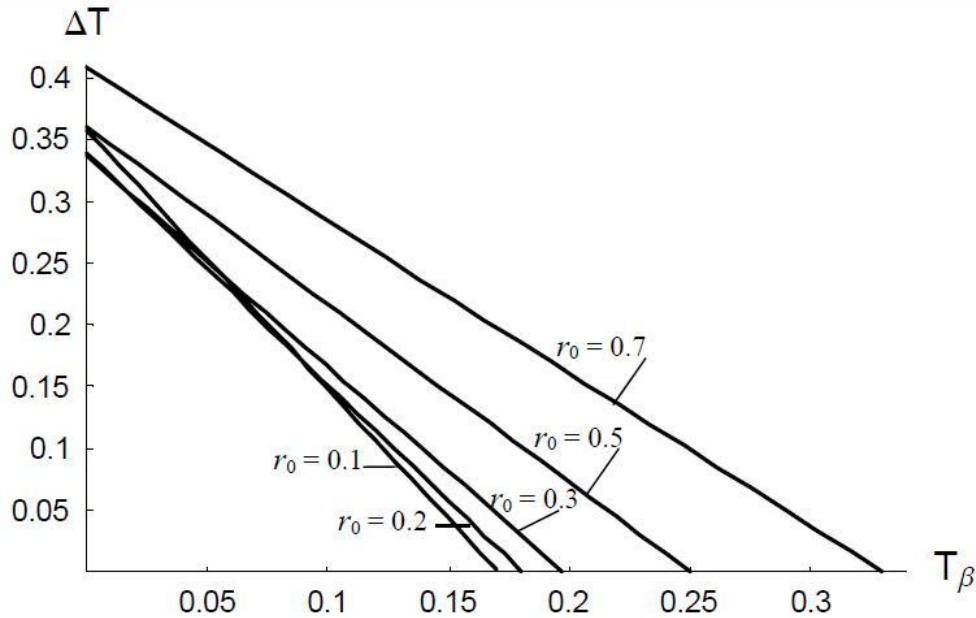


Fig. 3 Initiation of plastic yielding curves with two responsible parameters: fixed temperature at the outer radius and temperature differences (between inner and outer surfaces)

In the outer elastic zone, the kinematic analysis is straightforward and based on Eqs. (15), (19) and (7) with parameter ϕ_γ derived from Eqs. (20)-(21) for the same values of temperature parameters T_β , ΔT and geometric ratio r_0 .

6. Results and discussion

Numerical calculations are performed for a typical mild steel with the following mechanical properties: $Y=219.97$ MPa, $E=200$ GPa, $\alpha=18 \times 10^{-6}/^\circ\text{C}$ and three temperature parameters ① $T_\beta=\Delta T=0.15$, ② $T_\beta=\Delta T=0.30$ and ③ $T_\beta=\Delta T=0.45$. The temperature distributions along the radius are shown in Fig. 2. It is worth noting that, in contrast to the pressure vessels with similar logarithmic temperature gradients but free of stress boundary conditions and no displacement restraints (Harvey 1985), the elastic carrying capacity of constrained annular plate depends both on the uniform temperature distribution (initial fixed temperature at the outer radius) and temperature differences as shown in Fig. 3 for various inner radii.

To compare these results with the ones obtained from the assumption of the dependence of mechanical properties on temperature (Alexandrov *et al.* 2014), the relative increase in temperature, namely, the parameter $(T_{\beta p}-T_{\beta e})/T_{\beta e}$ as a function of dimensionless inner radius r_0 for several values of temperature mismatches ΔT is plotted in Fig. 4 where $T_{\beta p}$ is the temperature at the outer radius corresponding to the loss of load carrying capacity and $T_{\beta e}$ is the temperature at the outer radius corresponding to the elastic carrying capacity. It is seen from this figure that the curve for $\Delta T=0.3$ has a maximum corresponding to $r_0=0.28$. This curve has the same shape as the curves published by Alexandrov *et al.* (2014).

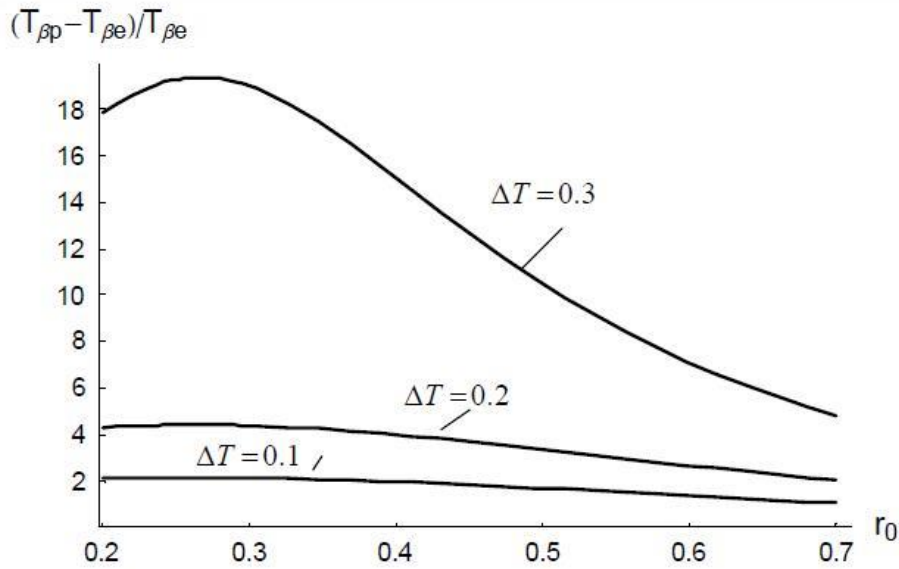


Fig. 4 Relative increase in temperature parameter versus dimensionless inner radius for various values of temperature mismatches

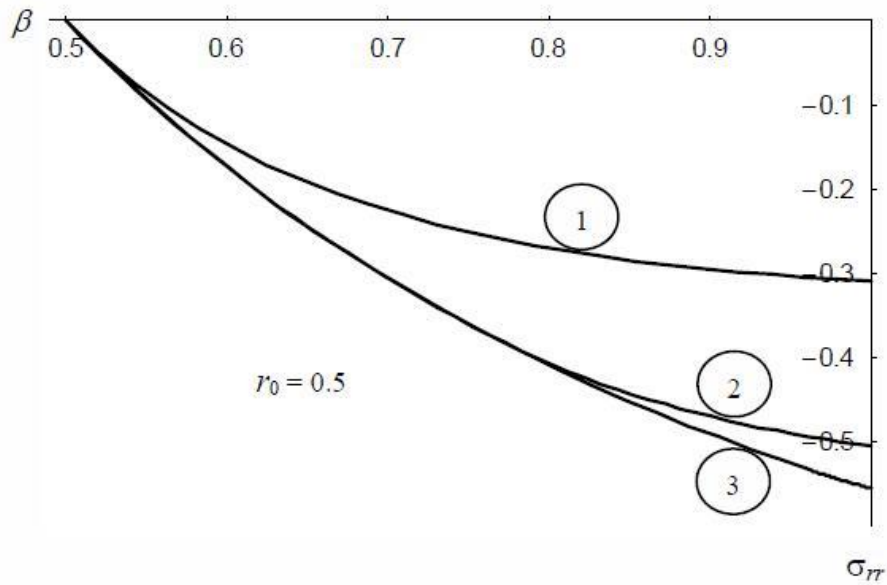


Fig. 5 Radial stress distributions for several variations of temperature parameters: 1- $T_{\beta} = \Delta T = 0.15$; 2- $T_{\beta} = \Delta T = 0.30$; 3- $T_{\beta} = \Delta T = 0.45$

When temperature at the inner surface T_a is positive, the radial stresses are compressive throughout the width of the plate and become zero at the inner surface as it is required by the stress boundary condition (Fig. 5). Circumferential stresses are also compressive but they behave differently in elastic state (curve 1) and plastic states (curves 2 and 3) as opposite to the same

behavior for the radial stresses (Fig. 6). For elastic state, the maximum circumferential stress is reached at the inner surface but, in plastic state, the maximum values are observed at the elastic plastic border. Particularly, the negative stress at the inner surface demonstrates the tendency for material to grow but it is then restricted by adjacent material at a lower temperature.

Moreover, plastic flow starts at the inner edge during the temperature loading, and plastic zone steadily propagates toward the outer surface. Finally, the plate becomes totally plastic in contrast to the pressurized annular plate embedded into a rigid container without temperature effects (Aleksandrova 2015).

The results of kinematic analysis are depicted in Figs. 7-8 where the radial displacement and strain tensor components (radial and tangential), respectively, are plotted as a function of β .

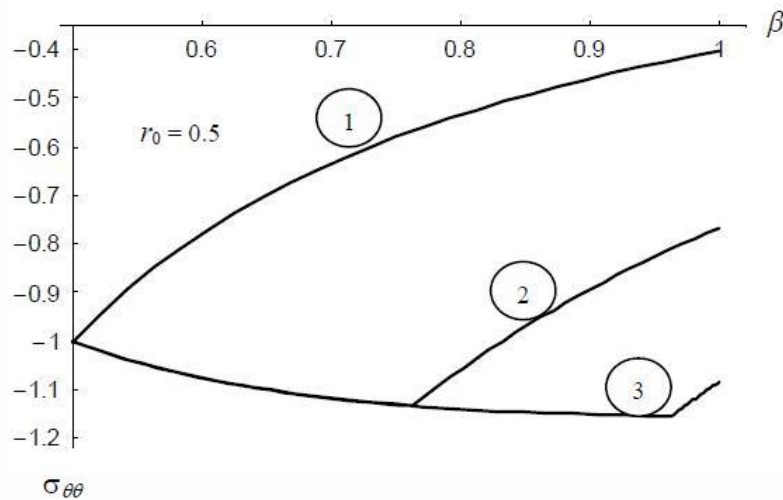


Fig. 6 Circumferential stress distributions for several variations of temperature parameters: 1- $T_{\beta}=\Delta T=0.15$; 2- $T_{\beta}=\Delta T=0.30$; 3- $T_{\beta}=\Delta T=0.45$

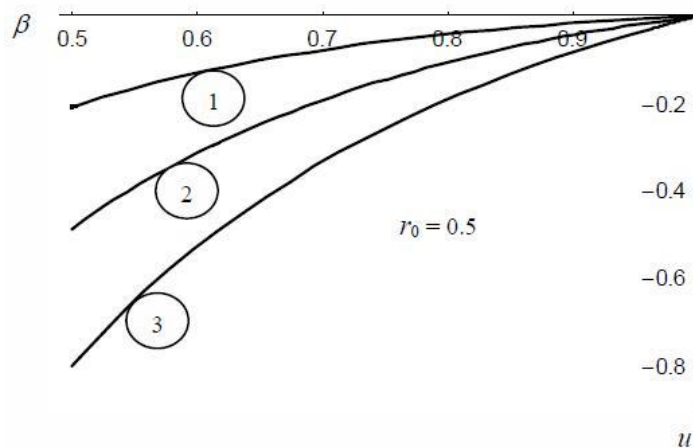


Fig. 7 Radial displacements for for several variations of temperature parameters: 1- $T_{\beta}=\Delta T=0.15$; 2- $T_{\beta}=\Delta T=0.30$; 3- $T_{\beta}=\Delta T=0.45$

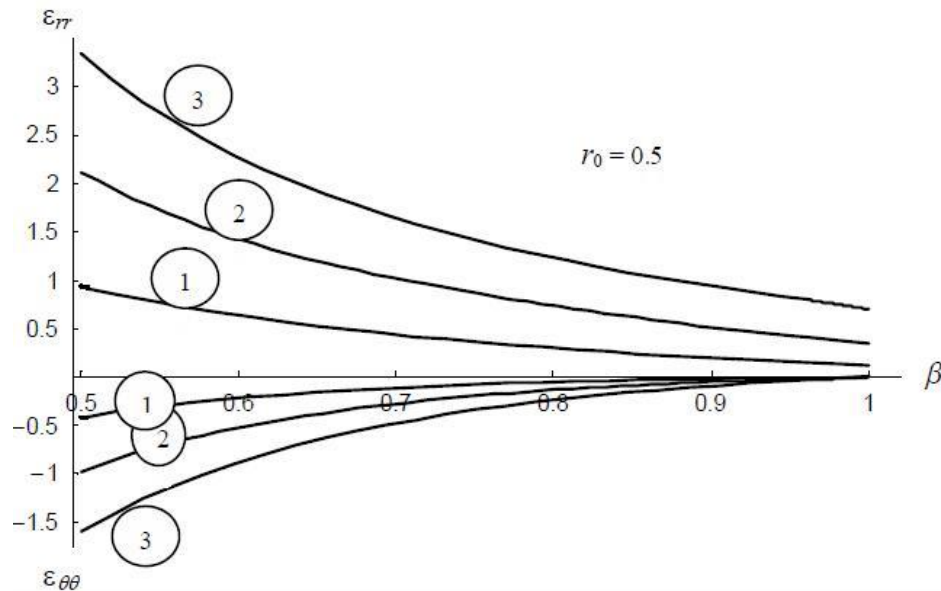


Fig. 8 Radial and tangential strain distributions for several variations of temperature parameters: 1- $T_{\beta} = \Delta T = 0.15$; 2- $T_{\beta} = \Delta T = 0.30$; 3- $T_{\beta} = \Delta T = 0.45$

It is interesting to note that the displacements are distributed evenly between purely elastic and plastic states, and reach maximum values at the inner surface. This fact manifests that the most probable mechanism of failure in the outer-radius constrained plates with temperature gradient is the loss of load carrying capacity rather than the loss of decohesive carrying capacity, that is the plate gets fully plastic first rather than experiences discontinuity due to the separation of the plate material from the rigid container. This is also confirmed by the radial strain distributions (Fig. 8) which are positive but finite in contrast to the positive infinite radial strains in the similar problems of annular plates with rigid inclusion where the decohesive carrying capacity occurs first and is the leading mechanism of failure (Szuwalski 1990). The tangential strains are negative and as much as two times less than the radial ones.

7. Conclusions

An extension of the constrained at the outer-radius annular plate subjected to uniform temperature field is presented to investigate the effect of radial logarithmic temperature gradient on the stress/strain distributions. The closed form solution is obtained which permits to analyze various thermal, mechanical and geometrical parameters involved in the process such as initial temperature, temperature differences, Poisson coefficient, inner to outer radius ratio of the plate. The main results of the study are as follows:

- The most probable mechanism of failure is the loss of load carrying capacity;
- Both elastic and load carrying capacities depend on geometric ratio (inner to outer radius) and Poisson coefficient;
- Plastic yielding provokes the flow of the material from the inner edge but simultaneously this

flow has the tendency to be restricted by an adjacent material at a lower temperature.

- At the inner surface, the displacements reach maximum (negative) value and then steadily vanish at the outer radius for whole course of temperature loading.

References

- Aleksandrova, N. (2015), "Engineering stress solutions for bolted and pressurized steel structures", *Struct.*, **1**, 60-66.
- Alexandrov, S. (2015), *Elastic/Plastic Discs Under Plane Stress Conditions*, Springer Briefs in Computational Mechanics, Springer International Publishing.
- Alexandrov, S. and Alexandrova, N. (2001), "Thermal effects on the development of plastic zones in thin axisymmetric plates", *J. Strain. Anal.*, **36**(2), 169-176.
- Alexandrov, S. and Pham, C. (2014), "Plastic collapse mechanism in thin disks subject to thermo-mechanical loading", *Asia Pacific J. on Comput. Eng.*, **1**, 7.
- Alexandrov, S., Wang, Y.C. and Aizikovich, S. (2014), "Effect of temperature-dependent mechanical properties of plastic collapse of thin discs", *Proc. IMechE Part C. J. Mechanical Engineering Science*, **228**(14), 2483-2487.
- Bland, D.R. (1956), "Elastoplastic thick-walled tubes of work-hardening material subject to internal and external pressures and to temperature gradients", *J. Mech. Phys. Solid.*, **4**, 209-229.
- Chakrabarty, J. (2006), *Theory of plasticity*, 3rd Edition, Elsevier Butterworth-Heinemann.
- Eraslan, A.N. and Apatay, T. (2008), "Analytical solution of nonlinear strain hardening preheated pressure tube", *Turkish J. Eng. Env. Sci.*, **32**, 41-50.
- Harvey, J.F. (1985), *Theory and Design of Pressure Vessels*, Van Nostrand Reinhold Company Inc., New York.
- Sen, F. and Sayer, M. (2006), "Elasto-plastic thermal stress analysis in a thermoplastic composite disc under uniform temperature using FEM", *Math. Comput. Appl.*, **11**(1), 31-39.
- Szuwalski, K. (1990), "Decohesive carrying capacity in perfect and asymptotically perfect plasticity", *Mechanika Teoretyczna I Stosowana*, **28**(1-2), 243-254.
- Timoshenko, S.P. and Goodier, J.N. (1970), *Theory of Elasticity*, 3rd Edition, McGraw-Hill, New York.
- Ugural, A.C. and Fenster, S.K. (2012), *Advanced Mechanics of Materials and Applied Elasticity*, 5th Edition, Prentice Hall, New York.
- Ventsel, E. and Krauthammer, T. (2001), *Thin Plates and Shells: theory, analysis, and applications*, Marcel Dekker, New York.
- Vullo, V. (2014), *Circular Cylinders and Pressure Vessels: Stress Analysis and Design*, Springer Series in Solid and Structural Mechanics, Vol. 3, Springer International Publishing.
- Zabaras, N., Mukherjee, S. and Arthur, W.R. (1987), "A numerical and experimental study of quenching of circular cylinders", *J. Therm. Stress.*, **10**, 177-191.
- Zhu, X.K. and Chao, Y.J. (2002), "Effects of temperature-dependent material properties on welding simulation", *Comput. Struct.*, **80**, 967-976.